THE BIOROBOTICS INSTITUTE

Sant'Anna School of Advanced Studies – Pisa

AIKIDO: Combining inverse kinematics and rigid constrained dynamics for online collision avoidance

Mattia Penzotti and Marco Controzzi

{mattia.penzotti, marco.controzzi}@santannapisa.it

The BioRobotics Institute and Department of Excellence in Robotics and AI, Scuola Superiore Sant'Anna, Pisa, Italy

ICRA IEEE INTERNATIONAL CONFERENCE ON ROBOTICS AND AUTOMATION

THE Tuscany Health Ecosystem Spoke 9 (project number ECS 00000017)

Finanziato dall'Unione europea NextGenerationEU

Italiadomani

Ministero dell'Università e della Ricerca

Watch AIKIDO in action!

1. Introduction

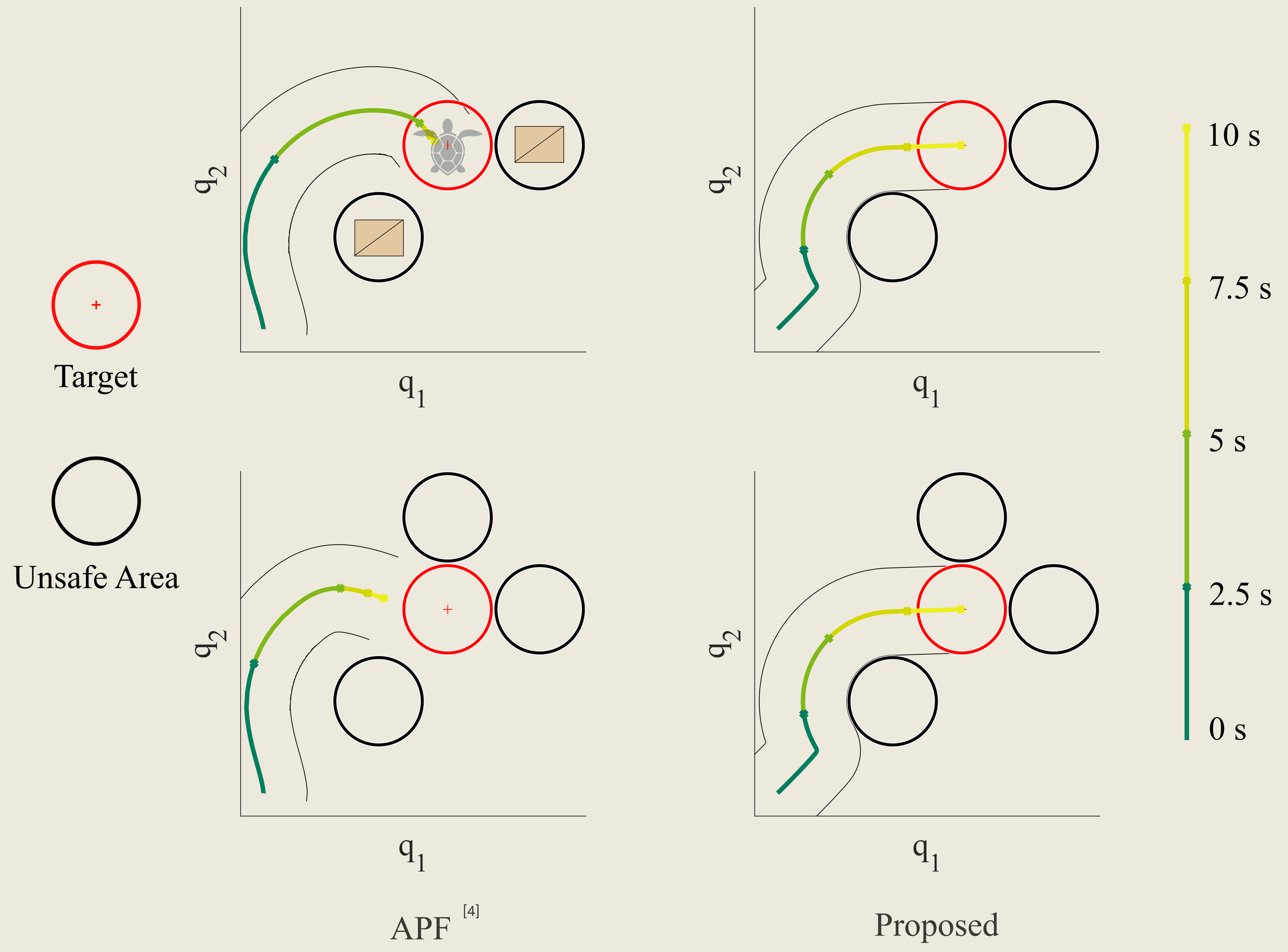

Artificial potential fields (APFs) are used for safety in operational space control by generating repulsive forces near obstacles [1]. Major limitations: causing oscillations when near obstacles or at high speeds, **affecting dynamics** away from unsafe areas [2], and needing **extensive tuning** to prevent local minima [3][4]. Our proposed approach, AIKIDO, aims to **maximize accuracy and minimize tuning efforts** to achieve arbitrarily safe motion.

2. Preliminaries

The **collision scene geometry**, plus the definition of a clearance value, naturally encodes in maximal coordinates **safe and unsafe** configurations and control inputs.

Our key insight is that we can leverage iterative dynamics to **test control inputs** before applying them to the real system.

The **clearance value** acts as an exact tunable (even at runtime) safety margin. It defines the minimum allowable distance between collision shapes (e.g., a link and an obstacle).

In a receding horizon fashion, we can **iteratively predict** near-future feasible states adhering closely to control inputs, up to necessary corrections (**distance constraints**).

3. Concept

1 Compute unconstrained (desired) velocities [5]

$$\dot{\mathbf{q}}_d = KJ^{\dagger}\phi + B(\tilde{\mathbf{q}} - \mathbf{q})$$

2 Infer near-future plausible state [6][7]

$$X^+ = X + VT + M^{-1}J_N^{\top}T^2\lambda$$

3 Derive optimal control action [8]

$$\min_{\mathbf{x}(t),\mathbf{u}(t)} \int_0^T \mathbf{u}(t)^{\top}\mathbf{u}(t)\,dt$$

subject to:

$$\mathbf{x}(t) = \begin{bmatrix}\mathbf{p}(t)\\ \mathbf{v}(t)\end{bmatrix}, \quad \dot{\mathbf{x}}(t) = \begin{bmatrix}\mathbf{v}(t)\\ \mathbf{u}(t)\end{bmatrix}, \quad t \in [0, T]$$

$$\mathbf{x}(0) = \begin{bmatrix}\mathbf{q}\\ \dot{\mathbf{q}}\end{bmatrix}, \quad \mathbf{x}(T) = \begin{bmatrix}\mathbf{q}_{X^+}\\ 0\end{bmatrix}$$

4. Closing the loop

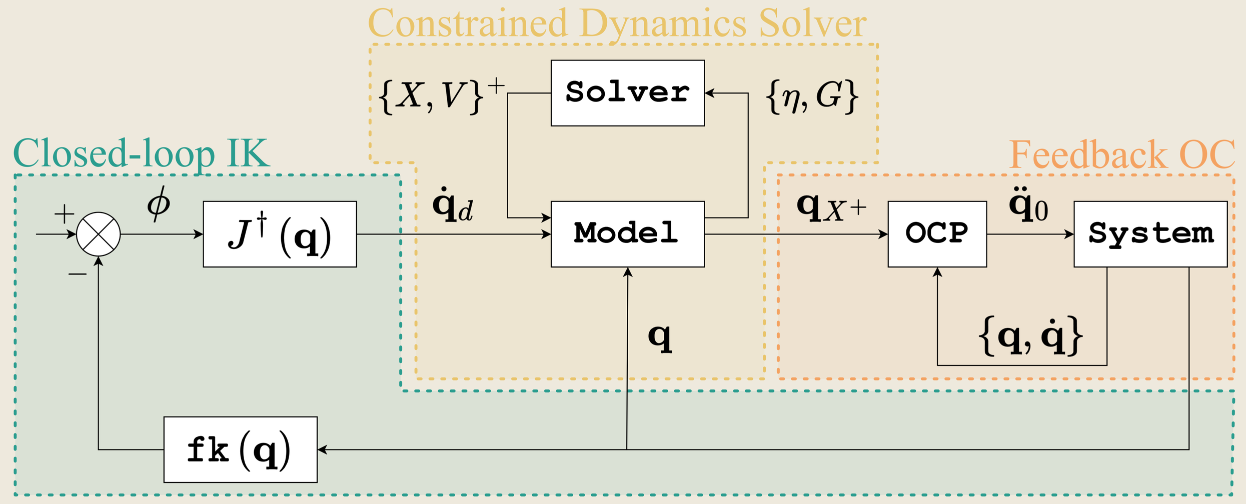

while controlling **do**
  $\mathbf{q}, \dot{\mathbf{q}} \leftarrow$ read()
  $\phi \leftarrow$ error() ▷ task space
  $\dot{\mathbf{q}}_d \leftarrow$ inverseKinematics($\phi, \mathbf{q}$) ▷ (10)
  $X \leftarrow X(\mathbf{q})$ ▷ reduced to maximal coordinates
  $V \leftarrow V(\dot{\mathbf{q}}_d)$ ▷ reduced to maximal coordinates
  $T_s \leftarrow \frac{T}{N}$
  updateCollisionModel() ▷ optional
  for $i = 1$ to N **do**
    $\eta, G \leftarrow$ evaluateModel(X, V) ▷ (7)
    $X, V \leftarrow$ evaluateSolver(η, G) ▷ (8), (9) with $T = T_s$
  end for
  $\mathbf{q}_{X^+} \leftarrow \mathbf{q}(X)$ ▷ maximal to reduced coordinates
  $\ddot{\mathbf{q}}_0 \leftarrow$ computeAction($\mathbf{q}, \dot{\mathbf{q}}, \mathbf{q}_{X^+}$) ▷ (15)
  write($\dot{\mathbf{q}} + \ddot{\mathbf{q}}_0\Delta t$)
end while

5. Simulation experiments

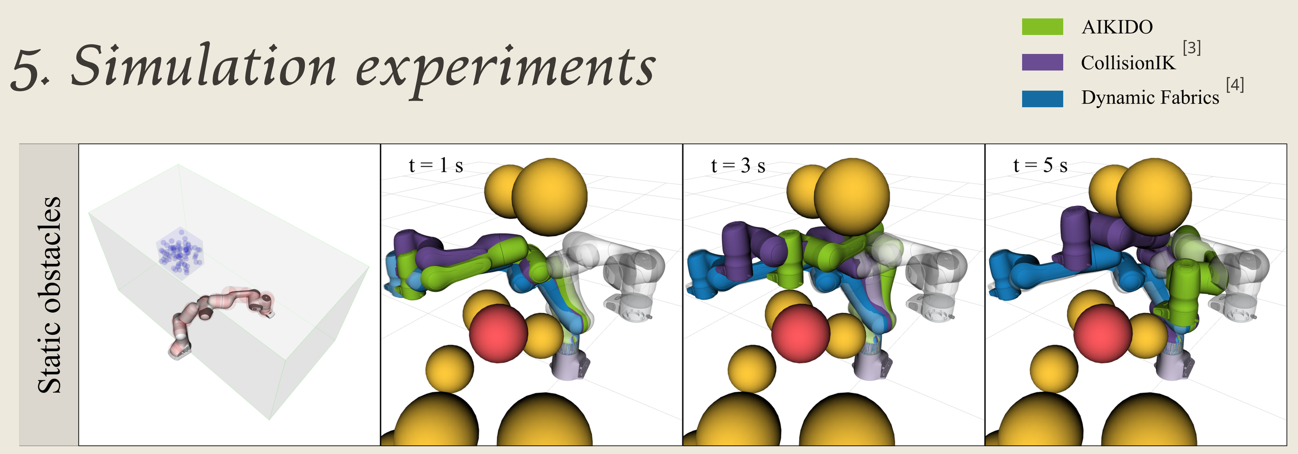

On the left, the home configuration (robot in solid colours), the end-effector workspace (transparent grey) and uniformly distributed position targets (transparent blue, transparent robot). For each trial, we **randomly generate obstacles** and select a target. A geometric RRT (global) planner [9] is then used to **validate the feasibility** of the trial. The global planner is constrained to maintaining a fixed end-effector orientation throughout the motion and to navigate **within the workspace**. The red sphere ensures that **no trivial solution** exists to accomplish the positioning task (in other words, some evading manoeuvres are required).

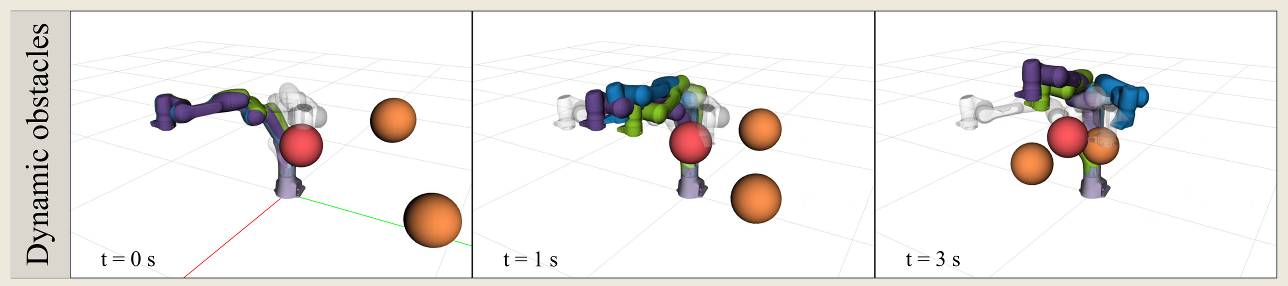

6. Metrics/Results

We use a simulated 7-DOF Franka Emika Panda robotic arm with a control rate of 100 Hz. For each scenario, we tested with an increasing number of spherically shaped obstacles (each with a radius of 0.1 m), up to a maximum of 15 obstacles. We conducted 80 trials for each condition, evaluating the performance in terms of **solver time** and **normalized travelled distance**, which were measured only for successful trials. A trial was deemed successful if the robotic arm reached the desired final position within a tolerance of 2 cm, **without any collisions**, and while adhering to all kinematic constraints of the simulated actuators (e.g., speed and position limits). To ensure that the trajectories generated by any of the compared planners were collision-free, we post-processed each configuration by calculating the closest-point distances between the robot and both static and dynamic obstacles. We set a timeout twice for the duration of the RRT motion plan.

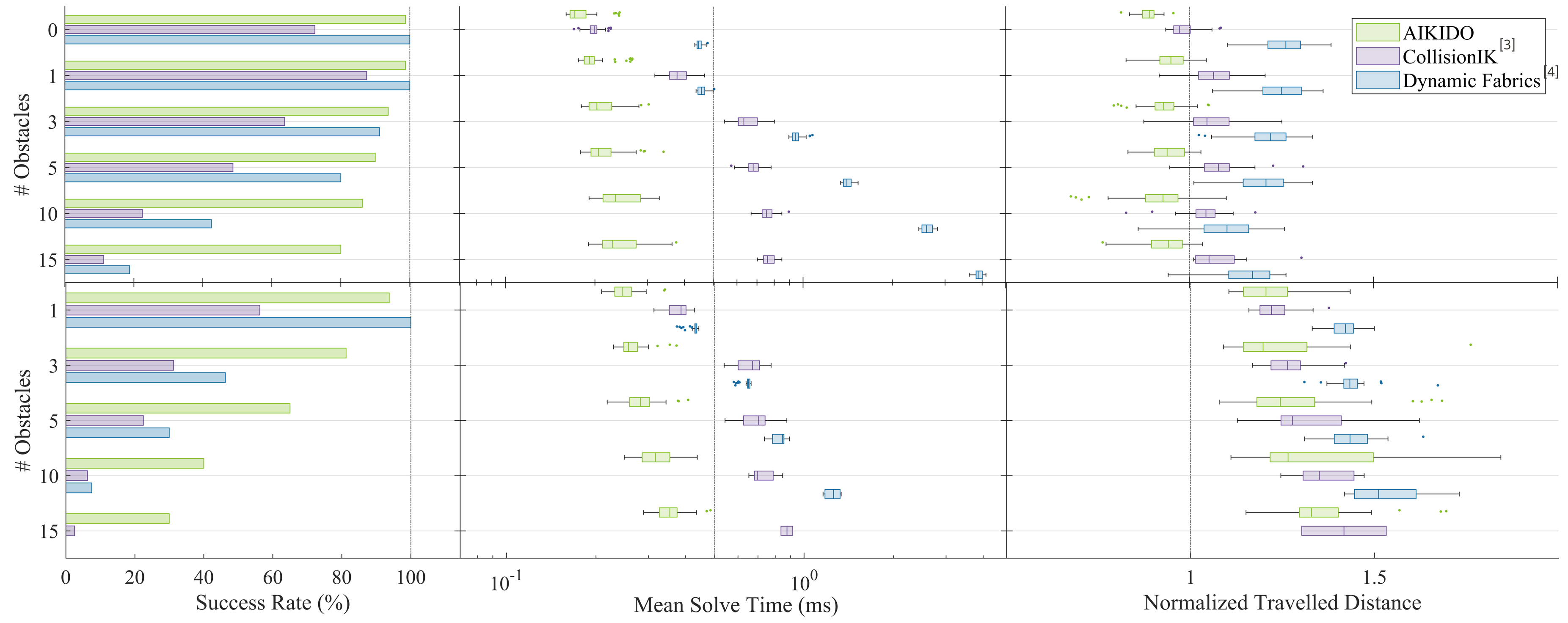

7. Real world evaluation

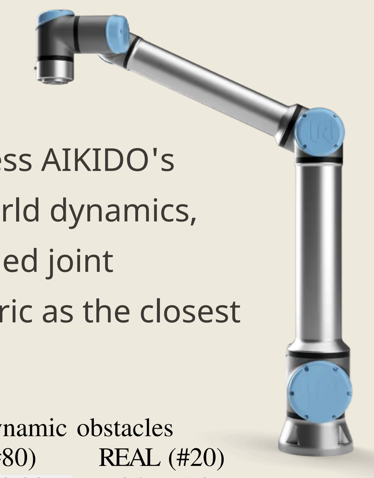

We conduct sim-to-real experiments on the UR10e to assess AIKIDO's closed-loop control performance with unmodeled real-world dynamics, considering **solver time**, **time to goal, action cost** (normed joint acceleration time integral), and **minimum clearance** metric as the closest point distance in successful trials.

	Wilcoxon (Z) or t-test (T)	Static obstacles SIM (#80)	Static obstacles REAL (#20)	Dynamic obstacles SIM (#80)	Dynamic obstacles REAL (#20)
Action cost		3.41 ± 0.72	3.42 ± 0.80	7.67 ± 3.20	7.34 ± 1.87
(rad/s^3)	T,p	0.03, 0.98		-0.41, 0.68	
Min. clearance		19.68 ± 2.00	18.50 ± 1.70	21.11 ± 2.82	21.12 ± 2.97
(mm)	Z,p	-1.74, 0.08		0.43, 0.66	
Time to goal		9.36 ± 0.76	9.25 ± 0.88	11.37 ± 2.06	11.39 ± 0.99
(s)	Z,p	-0.41, 0.68		-0.32, 0.75	
Solver time		0.51 ± 0.11	0.90 ± 0.04	0.63 ± 0.13	1.02 ± 0.05
(ms)	Z,p	6.09, <0.001***		6.31, <0.001***	
Success rate	-	0.73	0.80	0.81	0.85

Our closed-loop control scheme effectively manages unmodeled manipulator dynamics. Despite approaching the obstacle avoidance problem geometrically, we observe **no performance differences** between real-world and simulation experiments. Consistency is indicated by maintained clearance values (safety margin) during tasks.

08. Conclusions

In the present work, we propose a novel approach to local motion synthesis, which combines closed-loop inverse kinematics, rigid constrained dynamics and optimal control to overcome limitations of state of the art methods. In particular, we demonstrate **unmatched motion accuracy in the proximity of obstacles and self-collisions**, which enables our method to exhibit superior performances in challenging, general-purpose, arm positioning tasks.

[1] Khatib. The international journal of robotics research 5.1 (1986): 90-98.
[2] Duhé. Fractional Calculus and Applied Analysis 24 (2021): 421-446.
[3] Rakita. 2021 IEEE International Conference on Robotics and Automation (ICRA). IEEE, 2021.
[4] Spahn. IEEE Transactions on Robotics 39.4 (2023): 2684-2699.
[5] Colomé. IEEE/ASME Transactions On Mechatronics 20.2 (2014): 944-955.
[6] Catto. Game developer conference. Vol. 2. No. 5. 2005.
[7] Featherstone. Rigid body dynamics algorithms. Springer, 2014.
[8] Ghazaei. 2015 IMA Conference on Mathematics of Robotics. 2015.
[9] LaValle. Algorithmic and computational robotics (2001): 303-307.